Performance Analysis of a Kirigami-shaped Temperature Sensor

Nafize Ishtiaque Hossain
Department of Electrical
Engineering
The University of Texas at Tyler
Tyler, Texas, USA
nhossain2@patriots.uttyler.edu

Shawana Tabassum
Department of Electrical
Engineering
The University of Texas at Tyler
Tyler, Texas, USA
stabassum@uttyler.edu

Abstract—This work reports a kirigami-shaped sensor interfaced with an internet-of-things platform for strain insensitive and real-time temperature detection. The performance of the sensor was characterized under different stretching and twisting deformations, along with humidity variations. Excellent agreement was observed between the experimental and simulation results. The kirigami architecture shielded the sensor from motion artifacts, thereby demonstrating its promise in long-term wearable applications.

Keywords—kirigami, temperature sensor, gold nanoparticles, multiwalled carbon nanotube, wearable sensor, Internet-of-things

I. Introduction

Kirigami is a Japanese art of cutting and folding papers. Unlike origami that solely involves folding, kirigami also includes cutting. Kirigami-inspired architectures have opened a new dimension of sensing [1], energy harvesting [2], micro/nanophotonics [3], and super capacitance [4]. These structures are particularly suitable for creating complex three-dimensional (3D) objects from a planar 2D geometry. Through strategic cutting and folding mechanisms, kirigami structures can be made adaptive, reconfigurable, and strain invariant [3]. While several studies report promising applications of kirigami, their fabrication techniques rely mostly on photolithography [5] and focused ion beam irradiation [6]. In contrast, we used a facile and cost-effective synthesis procedure to create the kirigami sensing device.

This work reports a strain-insensitive temperature sensor formed on a kirigami framework. The kirigami device was subsequently interfaced with an Internet of Things (IoT)enabled data acquisition system for data processing and remote monitoring. The temperature sensor was made from a thin mesh of multi-walled carbon nanotube (MWCNT) embedded with gold nanoparticles (AuNPs). The AuNPs-MWCNT coating exhibited a negative temperature coefficient of resistance in response to variations in temperature. The kirigami network was composed of two bendable and twistable bridges at the opposite ends of an island. The temperature sensor on the island experienced minimum stress owing to the out-of-plane buckling of the kirigami bridges. The temperature sensor was further characterized for different tensile and torsional strains. Both experimental and simulation results demonstrated minimum stress induced on the sensor, yet the sensor showed high

wearable devices, which frequently suffer from structural deformations owing to varying degrees of motion artifacts.

II. DEVICE ARCHITECTURE

sensitivity to temperature changes. Therefore, sensors integrated

with a kirigami architecture find promising applications in

A. Fabrication of the Kirigami Sensor

First, the Kirigami patterns were engraved in a 125 μ m-thick polyimide sheet via a craft cutter [7], as illustrated in Fig. 1a. Each kirigami device was composed of two bridges hanging from a square-shaped island. Each bridge was made of an array of slits and notches. Subsequently, a temperature sensor was made on the island. To realize the sensor, the entire kirigami device was first coated with conductive graphene ink followed by the island coated with a thin layer of AuNPs-MWCNT. The preparation of the AuNPs-MWCNT coating is described elsewhere [8]. Fig. 1b shows the process flow for fabricating the temperature sensor. The dimension of the overall device was 7.3 cm by 1.1 cm, with the square-shaped island being 1 cm² and each slit being 0.1 cm wide under the relaxed state.

B. Interfacing with IoT-enabled Data Acquisition

The kirigami device was integrated with an ESP32 microcontroller unit to realize a standalone system (Fig. 2a). The microcontroller had a built-in WiFi module for transmitting data to the cloud (Fig. 2b). A voltage divider was used to detect the resistance variations of the temperature sensor and send those measurements to the microcontroller (Fig. 2c). Subsequently, the measured resistance was compared with a previously loaded

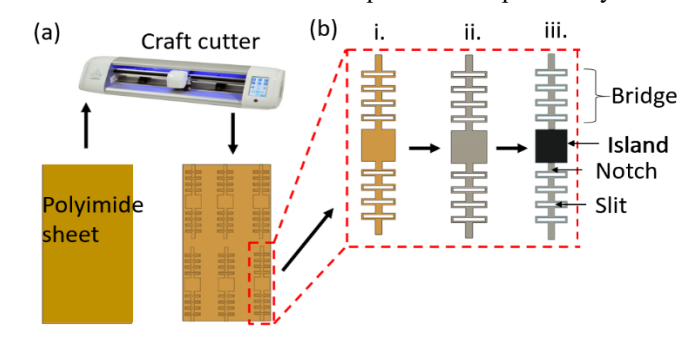


Fig. 1. (a) Polyimide sheet patterned into Kirigami slits and notches. (b) Temperature sensor fabrication flow: i. kirigami structure removed from the polyimide substrate, ii. graphene ink coated over the Kirigami shape and cured at 100°C for 60 minutes, iii. AuNPs-MWCNT coating deposited on the island.

This work was supported in part by VentureWell Grant No. 21716-20 and in part by the National Science Foundation Award No. 2138701.

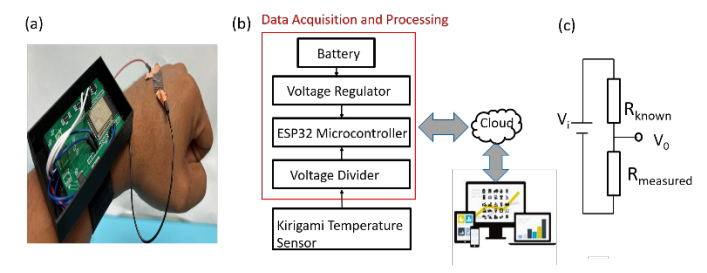


Fig. 2. (a) Complete system with IoT integration. (b) System architecture wherein the Kirigami sensor was interfaced with data acquisition and processing module via a (c) voltage divider circuit. The onboard Wi-Fi module transmitted the data wirelessly to the IoT cloud.

calibration curve to extract the unknown temperature reading. The temperature readings were sent to the cloud for further processing and remote monitoring.

III. STRESS AND STRAIN SIMULATION

Finite element analysis was used to investigate the stress-strain behavior of the kirigami device with the commercial COMSOL Multiphysics software. Fig. 3a demonstrates the surface von Mises stress distribution on the kirigami architecture. It was evident that for an applied strain of 20%, the kirigami notches experienced maximum stress of approximately 3 N/m², while the kirigami island encountered minimal stress. These results confirm that the sensor located on the island did not experience any substantial stress-induced deformations due to the stress cancellation effects of the surrounding kirigami bridges. Fig. 3b shows the simulated stress-strain plot, with the break point occurring at around 135% tensile strain.

IV. PERFORMANCE ANALYSIS

A. Temperature Sensor Subjected to Stretching and Twisting
The temperature sensor was subjected to different degrees of

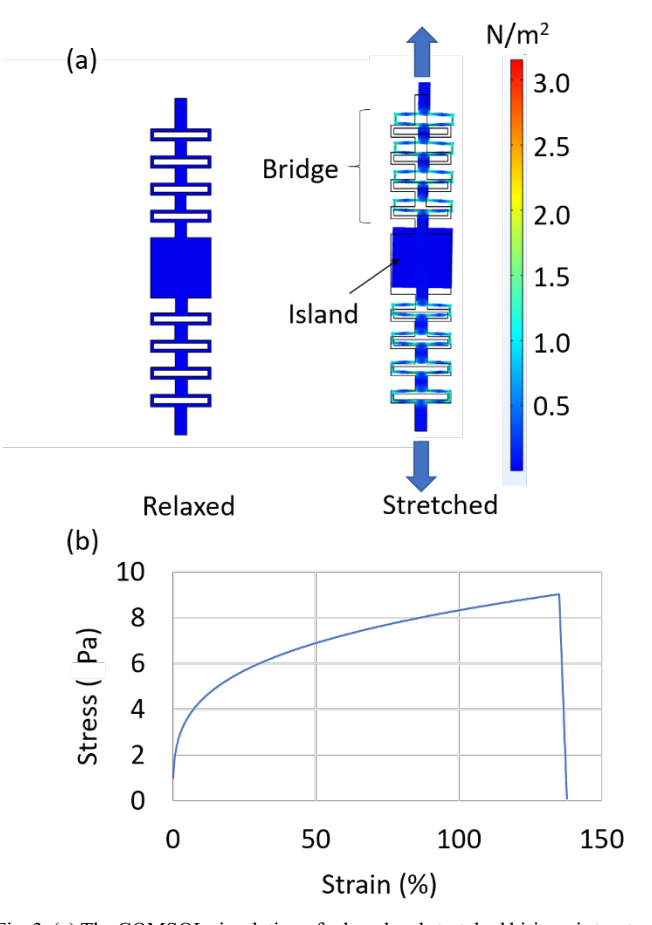


Fig. 3. (a) The COMSOL simulation of relaxed and stretched kirigami structure. The Kirigami bridges under stretched conditions experience higher stress as compared to the island, where the sensor is located. (b) The stress-strain plot.

stretching and twisting. In addition, a comparative analysis was conducted for resistance measured across the kirigami bridges (Fig. 4a) versus the resistance measured from the kirigami

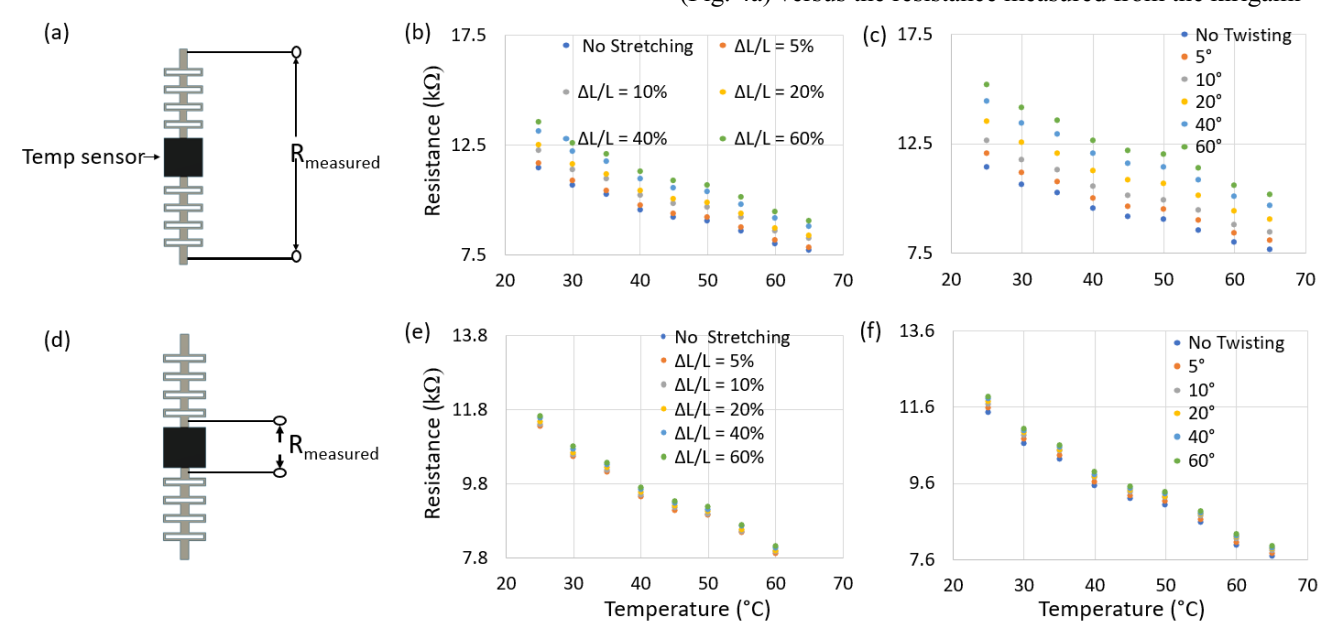


Fig. 4. (a) Resistance measured across the kirigami bridges. The resulting variations in resistance are shown under different amounts of (b) stretching and (c) twisting. (d) Resistance measured from the kirigami island. The resulting variations in resistance are shown under different amounts of (e) stretching and (f) twisting.

island (Fig. 4d). For an applied tensile strain ranging from 5% to 60%, a significant variation in the sensor response was observed with the resistance measured across the kirigami bridges (Fig. 4b). Similar variation was observed under twisting from 5° to 60° (Fig. 4c). In contrast, when the resistance was measured at the kirigami island, a negligible variation in resistance was observed under different degrees of stretching (5% to 60% in Fig. 4e) and twisting (5° to 60° in Fig. 4f). These results confirm that the kirigami architecture redistributed the strain to the slits and notches so that the sensor experienced nearly null stress. The resistance measurements from the sensor were further processed by a microprocessor to estimate the temperature from the previously loaded calibration curve.

B. Temperature Sensor Subjected to Different Humidity Conditions

The temperature sensor was tested under varying humidity conditions. The calibration plot had a slope of -0.0898 K Ω / 0 C and intercept of 13.405 K Ω for 60% RH and a linear temperature range (from T= 25 to 65 0 C). It was observed that at a fixed temperature, the resistance measured across the sensor decreased with increasing relative humidity (RH). Fig. 5 demonstrates shifts in the calibration curve of the temperature sensor in response to variations in RH. Therefore, the calibration curve of the temperature sensor was corrected for humidity variations using the following equations [9, 10]:

$$f_{slope} = \frac{Slope_{X\%RH}}{Slope 60\%RH} \tag{1}$$

$$f_{intercept} = \frac{Intercept_{X\%RH}}{Intercept 60\%RH}$$
 (2)

where f_{slope} and $f_{intercept}$ are the correction factors for slope and intercept of the sensor's calibration curve, respectively. Slopex%RH and Slope60%RH are slopes of the calibration curve at unknown RH and reference RH, respectively. Interceptx%RH and Intercept60%RH are intercepts of the calibration curve at unknown RH and reference RH, respectively.

Furthermore, the sensor was subjected to two variables simultaneously. For instance, Fig. 6a shows the response of the sensor under stretching and humidity variations, while Fig. 6b shows the response of the sensor under twisting and humidity variations. The results are commensurate with the findings shown in Fig. 4 and 5.

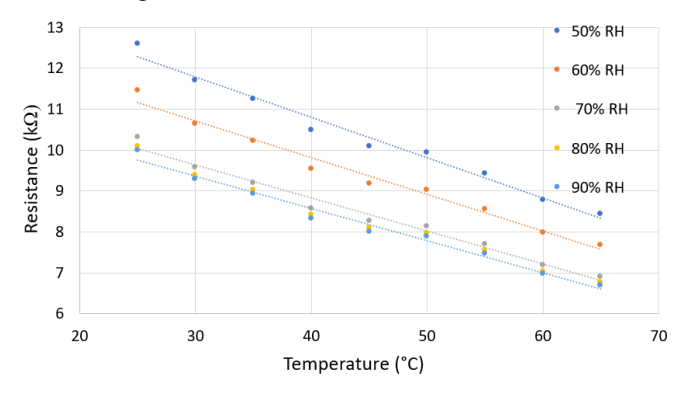


Fig. 5. Calibration curves of the temperature sensor under different relative humidity conditions.

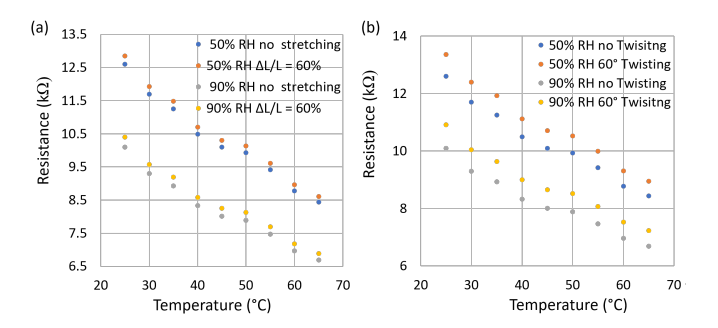


Fig. 6. Calibration curves of the temperature sensor under different (a) stretching and (b) twisting conditions at two different RH values.

V. CONCLUSION

In summary, this work reports a kirigami-structured temperature sensor coated with a highly sensitive AuNPs-MWCNT layer. The sensor demonstrated a highly stable performance under large strain variations, which was confirmed by both experimental results and finite element analysis-based simulation. In addition, the IoT integration makes the system integrated and compact, expanding its application to wearable settings.

REFERENCES

- K. Xu, Y. Lu, S. Honda, T. Arie, S. Akitaa, and K. Takei, "Highly stable kirigami-structured stretchable strain sensors for perdurable wearable electronics," *J. Mater. Chem. C*, vol. 7, pp. 9609-9617, Jul 2019.
- [2] Z. Xu, C. Jin, A. Cabe, D. Escobedo, A. Gruslova, S. Jenney, A. B. Closson, L. Dong, Z. Chen, M. D. Feldman, and J. X. J. Zhang, "Implantable cardiac kirigami-inspired lead-based energy harvester fabricated by enhanced piezoelectric composite film," Adv. Healthc. Mater., vol. 10, pp. e2002100, Jan 2021.
- [3] Z. Liu, H. Du, J. Li, L. Lu, Z. -Y. Li, and N. X. Fang, "Nano-kirigami with giant optical chirality," Sci. Adv., vol. 4, pp. eaat4436, Jul 2018.
- [4] R. Xu, A. Zverev, A. Hung, C. Shen, L. Irie, G. Ding, M. Whitmeyer, L. Ren, B. Griffin, J. Melcher, L. Zheng, X. Zang, M. Sanghadasa, and L. Lin, "Kirigami-inspired, highly stretchable microsupercapacitor patches fabricated by laser conversion and cutting," *Microsystems & Nanoengineering*, vol. 4, 2018.
- [5] S. Chen, J. Chen, X. Zhang, Z. -Y. Li, and J. Li, "Kirigami/origami: unfolding the new regime of advanced 3D microfabrication/nanofabrication with folding," Light: Science Applications, vol. 9, no. 75, pp. 1-19, April 2020.
- [6] D. Xia and J. Notte, "Nano-kirigami structures and branched nanowires fabricated by focused ion beam-induced milling, bending, and deposition," Adv. Mater. Interfaces, pp. 2200696, July 2022.
- [7] T. Noushin, N. I. Hossain, and S. Tabassum, "Kirigami-patterned highly stable and strain insensitive sweat pH and temperature sensors for longterm wearable applications," in proc. IEEE Healthcare Innovations and Point of Care Technologies (HI-POCT), pp. 108-111, March 2022.
- [8] T. Noushin, N. I. Hossain, and S. Tabassum, "IoT-enabled integrated smart wound sensor for multiplexed monitoring of inflammatory biomarkers at the wound site," Front. Nanotechnol., vol. 4, pp. 851041, March 2022.
- [9] A. Wiorek, M. Parrilla, M. Cuartero, and G. A. Crespo "Epidermal patch with glucose biosensor: pH and temperature correction toward more accurate sweat analysis during sports practice" ACS Anal. Chem., vol. 92, pp. 10153–10161, 2020.
- [10] N. I. Hossain and S. Tabassum, "Stem:FIT: a microneedle-based multiparametric sensor for in situ monitoring of salicylic acid and pH levels in live plants," in proc. IEEE International Conference on Nano/Micro Engineered and Molecular Systems (NEMS), pp. 312-316, April 2022.